Eur. Phys. J. C 25, 459–464 (2002)
Digital Object Identifier (DOI) 10.1007/s10052-002-0994-y

THE EUROPEAN PHYSICAL JOURNAL C

MHD fluctuations and low energy solar neutrinos

M.M. Guzzo[1], P.C. de Holanda[1], N. Reggiani[2]

[1] Instituto de Física Gleb Wataghin, Universidade Estadual de Campinas, UNICAMP, 13083-970 Campinas SP, Brazil
[2] Faculdade de Matemática, Centro de Ciências Exatas, Ambientais e Tecnologias, Pontifícia Universidade Católica de Campinas, 13086-900 Campinas-SP, Brazil

Received: 2 July 2001 / Revised version: 4 April 2002 /
Published online: 20 August 2002 –

Abstract. We analyze here how future solar neutrino experiments could detect neutrino flux fluctuations due to magnetohydrodynamics (MHD) perturbations on the solar plasma. We state that if such time fluctuations are detected, this would provide a unique signature of the resonant spin-flavor precession (RSFP) mechanism as a solution to the solar neutrino problem.

1 Introduction

Assuming a non-vanishing magnetic moment for neutrinos, active solar neutrinos that are created in the Sun interact with the solar magnetic field and can be spin-flavor converted into sterile non-electron neutrinos or into active non-electron anti-neutrinos. In both cases the resulting particles interact with solar neutrino detectors significantly less than the original active electron neutrinos, in such a way that this phenomenon can induce a depletion in the detectable solar neutrino flux [1,2]. If this interaction of the neutrinos with the solar magnetic field is the mechanism that explains the neutrino deficit on Earth, or, in other words, if the spin-flavor precession (RSFP) is the mechanism that can solve the solar neutrino problem, neutrinos are necessarily very much sensitive to fluctuations of the solar magnetic field, and, in particular, solar magnetohydrodynamic (MHD) perturbations can lead to time fluctuations of the solar neutrino flux detected on Earth.

According to previous works which analyze the RSFP phenomenon [3], the low energy solar neutrinos, with $E = 1\,\mathrm{MeV}$, will be more sensitive to MHD fluctuations, with a typical period of the order of a few days. Some operating solar neutrino detectors that are sensitive to such an energy range, like Homestake [4], Gallex/GNO [5,6] and Sage [7] cannot detect these fluctuations because they do not operate in a real-time basis, and such small fluctuations will be averaged out over the detection time. The Super-Kamiokande [8] and SNO [9] detectors operate in real-time basis but have a too high threshold in the neutrino energy to be sensitive to such fluctuations. Therefore, it is necessary to consider the detectors that operate in a real-time basis and that have a low threshold in the neutrino energy, like Borexino [10], Hellaz [11] and Heron [12]. In the present paper we consider how these MHD perturbations can be seen by these experiments, taking into account experimental details like the cross-section and threshold. We concluded that no time fluctuation will be felt by the Borexino experiment, while the Hellaz and/or Heron experiment may be able to detect the time fluctuations on the neutrino signal generated by the MHD fluctuations.

2 MHD perturbations

The MHD perturbations were calculated deriving the MHD equations near the solar equator, the region relevant for solar neutrinos. Using cylindrical coordinates, considering also the effects of gravity, we obtained the Hain–Lüst equation with gravity [13,14]:

$$\frac{\partial}{\partial r}\left(f(r)\frac{\partial}{\partial r}(r\xi_r)\right) + h(r)\xi_r = 0, \tag{1}$$

where

$$f(r) = \frac{\gamma p + B_o^2}{r}\frac{(\omega^2-\omega_{\mathrm{A}}^2)(\omega^2-\omega_{\mathrm{S}}^2)}{(\omega^2-\omega_1^2)(\omega^2-\omega_2^2)}, \tag{2}$$

$$\begin{aligned} h(r) = {} & \rho_0\omega^2 - k^2B_0^2 + g\frac{\partial\rho_0}{\partial r} \\ & - \frac{1}{D}g\rho_0^2(\omega^2\rho_0 - k^2B_0^2)\left[gH + \frac{\omega^2}{r}\right] \\ & - \frac{\partial}{\partial r}\left[\frac{1}{D}\omega^2\rho_0^2 g(\omega^2\rho_0 - k^2B_0^2)\right], \end{aligned} \tag{3}$$

and

$$\omega_{\mathrm{A}}^2 = \frac{k^2B_0^2}{\rho_0}, \quad \omega_{\mathrm{S}}^2 = \frac{\gamma p}{\gamma p + B_0^2}\frac{k^2B_0^2}{\rho_0}, \tag{4}$$

$$\omega_{1,2}^2 = \frac{H(\gamma p + B_0^2)}{2\rho_0}$$

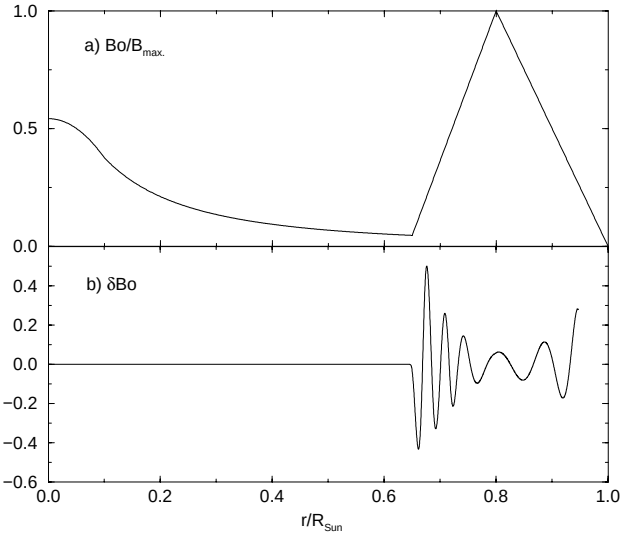

Fig. 1a,b. Results of MHD fluctuations on the magnetic field using a triangular profile in the convective zone: in **a** is shown the non-perturbed magnetic field profile B_0 normalized by its maximum value $B_{\max}$ as a function of the radial distance r normalized by the solar radius $R_{\rm Sun}$. In **b** the MHD fluctuations δB_0 are shown as a function of $r/R_{\rm Sun}$

$$\times \left\{ 1 \pm \left[1 - 4 \frac{\gamma p k^2 B_0^2}{(\gamma p + B_0^2)^2 H} \right]^{1/2} \right\}, \tag{5}$$

$$D = \rho_0^2 \omega^4 - H[\rho_0 \omega^2 (\gamma p + B_0^2) - \gamma p k^2 B_0^2], \tag{6}$$

$$H = \frac{m^2}{r^2} + k^2, \tag{7}$$

where ξ_r is the radial component of the plasma displacement ξ, g is the acceleration due to gravity, p is the pressure, $\gamma = C_p/C_v$ is the ratio of the specific heats, ρ_0 is the equilibrium matter density profile and B_0 is the magnetic equilibrium profile in the Sun. In this derivation we considered the equilibrium magnetic profile B_0 to be in the z direction.

The Hain–Lüst equation shows singularities when $f(r)$ given in (2) is equal to zero, that is, when $w^2 = w_{\rm A}^2$ or $w^2 = w_{\rm S}^2$, which regions in the w^2 space are called Alfvén and slow continua, respectively. In the interval $0 \leq r \leq 1$ the functions $w_{\rm A}^2$ and $w_{\rm S}^2$ take continuous values that define the ranges of the values of w^2 that correspond to improper eigenvalues, associated with localized modes. Eigenvalues of the Hain–Lüst equation must be searched, therefore, outside the regions where $w^2 = w_{\rm A}^2$ or $w^2 = w_{\rm S}^2$, and they define the global modes which are associated with magnetic and density waves along the whole radius of the Sun.

For the equations above we considered for the solar matter density distribution, ρ_0, and for the pressure p, the standard solar model prediction, that is, approximately monotonically decreasing exponential functions in the radial direction from the center to the surface of the Sun [15]. The density profile was used to calculate the acceleration of gravity. For the equilibrium magnetic profile we assumed a triangular configuration in the convective zone and an exponential decreasing profile in the center of the Sun. This magnetic profile is presented in Fig. 1a. We have chosen this profile because it gives a very good fit to the solar neutrino problem, as we will see in the next section.

The global modes were obtained solving numerically the Hain–Lüst equation with gravity, imposing appropriate boundary conditions to b_1 and ρ_1, the magnetic and density perturbations respectively, given by [13]

$$b_1 = \nabla \times (\xi \times B_0) \tag{8}$$

and

$$\rho_1 = \nabla \cdot (\rho \xi). \tag{9}$$

The matter density fluctuations were very constrained by helioseismology observations. The largest density fluctuations ρ_1 inside the Sun are induced by temperature fluctuations δT due to convection of matter between layers with different local temperatures. According to an estimate of such an effect [3], we assume density fluctuations ρ_1/ρ_0 smaller than 10%. The size of the amplitude b_1 is not very constrained by the solar hydrostatic equilibrium, since the magnetic pressure $B_0^2/8\pi$ is negligibly small when compared with the dominant gas pressure for the equilibrium profiles considered. Despite this fact, it cannot be arbitrarily large when we are solving the Hain–Lüst equation. This equation is obtained after linearization of the magnetohydrodynamics equations, which requires that the solution ξ must be very small, $|\xi| << 1$, so that the non-linear terms can be neglected. Moreover, we must have a clear distinction between the maximum and minimum magnetic field. In order to satisfy these criteria and have a significant effect, we choose the maximum value of the perturbation such that $|b_1|/|B_0| \sim 0.5$. In Fig. 1b we present a sample of a global MHD magnetic perturbation.

The period of the global modes that we obtained considering the equilibrium profiles and boundary conditions mentioned above is around 20 days [6].

3 Fitting the data

If we consider a non-vanishing neutrino magnetic moment, the interaction of such neutrinos with this magnetic field will generate neutrino spin-flavor conversion which is given by the evolution equations

$$\mathrm{i}\frac{\mathrm{d}}{\mathrm{d}r}\begin{pmatrix}\nu_{\rm L}\\ \nu_{\rm R}\end{pmatrix} = \begin{pmatrix} \frac{\sqrt{2}}{2}G_{\rm F}N_{\rm eff}(r) - \frac{\Delta m^2}{4E} & \mu_\nu |B_\perp(r)| \\ \mu_\nu |B_\perp(r)| & +\frac{\sqrt{2}}{2}G_{\rm F}N_{\rm eff}(r) + \frac{\Delta m^2}{4E} \end{pmatrix} \times \begin{pmatrix}\nu_{\rm L}\\ \nu_{\rm R}\end{pmatrix}, \tag{10}$$

where $\nu_{\rm L}$ ($\nu_{\rm R}$) is the left- (right-) handed component of the neutrino field, Δm^2 is the squared mass difference of the

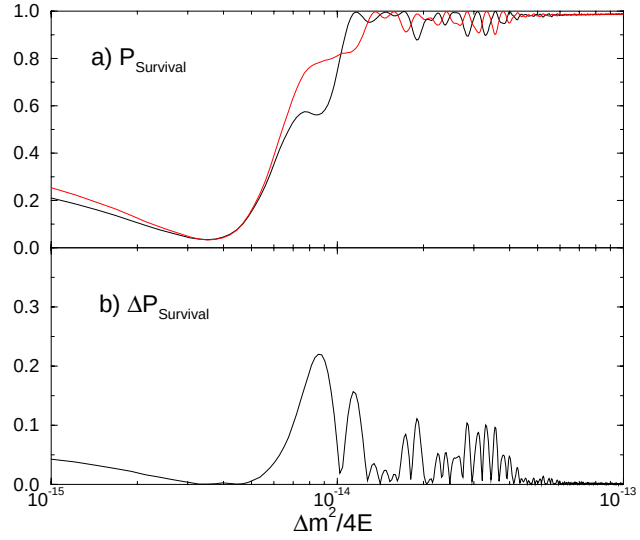

Fig. 2a,b. The neutrino survival probability $P_{\rm Survival}$, as a function of $\Delta m^2/4E$, for the maximum and the minimum of the MHD fluctuation, and **b** the fluctuations of the survival probability $\Delta P_{\rm Survival}$, caused by MHD perturbations, which is calculated as the difference of the two curves in **a**. We used here a triangular profile for the solar magnetic field on the convective zone

corresponding physical fields, E is the neutrino energy, $G_{\rm F}$ is the Fermi constant, μ_ν is the neutrino magnetic moment and $|B_\perp(r)|$ is the transverse component of the perturbed magnetic field. Finally, we have $N_{\rm eff} = N_e(r) - N_n(r)$ for Majorana neutrinos, where $N_e(r)$ ($N_n(r)$) is the electron (neutron) number density distribution, in which case the final right-handed states $\nu_{\rm R}$ are active non-electron antineutrinos. For Dirac neutrinos, $N_{\rm eff} = N_e(r) - 1/2N_n(r)$; in this case the right-handed final states are sterile non-electron neutrinos [5]. In this paper we will assume Majorana neutrinos. Note, however, that since $N_n \sim (1/6)N_e$ inside the Sun, the difference of taking Dirac or Majorana neutrinos leads to a multiplicative factor of $\sim 10/11$, and does not lead to sensible alterations in our conclusions, which are, in this way, valid for Majorana or Dirac neutrinos.

MHD magnetic and density fluctuations, b_1 and ρ_1, can alter the neutrino evolution since they can induce a time variation of the transverse component of the magnetic field $|B_\perp(r)|$ as well as the matter density $N_e(r)$ appearing in the evolution equation above. Therefore, the MHD fluctuations can induce a time variation on the survival probability of the neutrinos, that can be detected in the experiments on Earth. In Fig. 2 we present a sample of the effect of the MHD fluctuations on the survival probability of the neutrinos as a function of $\Delta m^2/4E$.

To analyze the results of these time fluctuations on specific experiments, it is necessary to establish exactly in which range of Δm^2 we are working. To do so, we made a general fit of the RSFP solution to the total rate of the present solar neutrino experiments, and restricted the range of Δm^2 into some confidence level region. Although this kind of fit was already done in recent papers [16–20], the magnetic field configurations we are using here are not exactly the same as the ones used in these papers (for instance, we have a non-zero inner magnetic field for the triangular configuration). So we chose to use our own results; moreover, they are in good agreement with the ones in [16–20].

In this fit procedure, we include the data of five solar neutrino detectors [4–7,**?**,9], where the latest data of the SNO detector were included. We also include Super-Kamiokande flux-independent information for taking into account any possible spectrum distortion or Earth regeneration effect. A similar procedure was also done in a recent work [19], where the RSFP mechanism was also analyzed with a somewhat different magnetic field profile.

A local best fit point for this configuration exist for $\Delta m^2 = 1.51 \times 10^{-8}\,{\rm eV}^2$, and $B_{\rm max} = 1.95 \times 10^5 (\times f_{B_0})G$, for a neutrino magnetic moment given by $\mu_\nu = 10^{-11}\mu_B$ $(/f_{B_0})$, and where $B_{\rm max}$ is the maximum value of the magnetic field in the convective zone, giving a $\chi^2_{\rm min} = 41.4$ for 46 degrees of freedom, which is a solution at $\sim 66\%$ C.L..

Our χ^2 function is defined as follows:

$$\chi^2 = \chi^2_{\rm R} + \chi^2_{\rm fi},$$

where $\chi^2_{\rm R}$ ($\chi^2_{\rm fi}$) relates to the total rates (flux-independent information) given by all experiments considered (Super-Kamiokande). These two contributions for the final χ^2 can be written as follows:

$$\chi^2_{\rm R} = \sum_{i,j=1,\ldots,5} \left[R_i^{\rm th} - R_i^{\rm obs}\right] \left[\sigma^2_{\rm R}\right]^{-1}_{ij} \left[R_j^{\rm th} - R_j^{\rm obs}\right], \quad (11)$$

where $R_i^{\rm th}$ and $R_i^{\rm obs}$ denote, respectively, the predicted and the measured value for the event rates of the five solar experiments considered. For the flux-independent contribution, we have

$$\chi^2_{\rm fi} = \sum_{i=1,44} [\alpha R^{\rm th}_{{\rm SK},i} - R^{\rm obs}_{{\rm SK},i}][\sigma_{\rm fi}(i,j)^2]^{-1}[\alpha R^{\rm th}_{{\rm SK},i} - R^{\rm obs}_{{\rm SK},i}], \quad (12)$$

where $R^{\rm th}_{{\rm SK},i}$ are the theoretically expected event rates for the ith bin computed by using the ^{8}B neutrino energy spectrum given in [21] normalized to the BP2000 SSM value [15], $R^{\rm obs}_{{\rm SK},i}$ is the corresponding observed rate reported by the SK Collaboration [8], α is a free parameter to avoid double-counting of the SK total rate in the statistical treatment, and $\sigma_{\rm fi}(i,j)$ is the 44×44 error matrix for the SK zenith-spectrum data.

We introduced a normalization factor f_{B_0} in both the magnetic field profile and in the neutrino magnetic moment. Since for neutrino oscillations the important quantity is $\mu_\nu \times B$, this factor does not change the quality of the fit or any quantity related to neutrino oscillations. But since the MHD equations depend only on B_0, this factor plays a crucial role in determining the profile of our MHD perturbations.

We will do our analysis considering a 99% C.L. region on the parameter space around the best fit point. According to our fit to the experimental data, this region allows us to vary the value of Δm^2 in the range $[1.0–2.2] \times 10^{-8}\,{\rm eV}^2$.

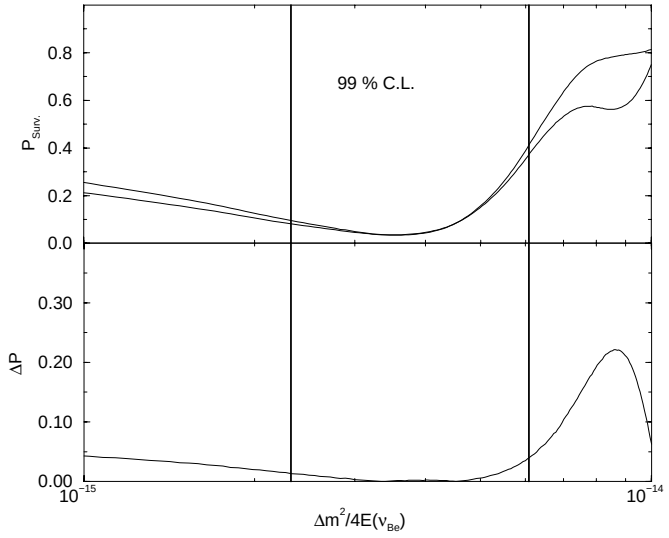

Fig. 3. Time fluctuations expected to the beryllium line, to be seen in Borexino experiment. The vertical lines correspond to the region within the beryllium line will fall with 99% C.L., according to the values obtained to Δm^2 with our fit procedure

4 Results

We will now analyze the effects of MHD fluctuations on different future experiments. In Fig. 2 it can be seen that when $\Delta m^2/4E \sim 10^{-14}\,\mathrm{eV}$ there is a fluctuation of the order of 10% of the detectable neutrinos. Considering that the best fit of the RSFP solution to the solar neutrino problem was obtained for $\Delta m^2 \sim 10^{-8}\,\mathrm{eV}^2$ we conclude that neutrinos with an energy of the order of 1 MeV will be very sensitive to MHD fluctuations if the RSFP phenomenon is the solution of the solar neutrino anomaly. Solving the Hain–Lüst equation with gravity we obtained the result that the period of oscillations of the MHD fluctuations are of the order of 20 days. Such fluctuations can only be detected in real-time experiments, otherwise they would be averaged out over the detection time. Therefore, it is necessary to consider the effect of these fluctuations on low energy and real-time experiments, like Borexino, Hellaz and Heron.

The Borexino experiment

This experiment [10] will be able to measure the beryllium line neutrinos, in a real-time basis. Since the beryllium neutrinos have a fixed energy ($E = 0.863\,\mathrm{MeV}$), it is quite easy to predict the time dependence of the neutrino signal in Borexino for a given Δm^2, just reading it directly from Fig. 2. Fixing the neutrino energy and taking the magnetic field normalization $f_{B_0} = 5$, we present in Fig. 3 the position of the beryllium line at 99% C.L. We show the survival probability P_{surv} at the maximum and at the minimum RSFP and the corresponding ΔP_{surv} difference. Inside this C.L. region, no reasonable time fluctuation will be felt by this experiment.

This behavior occurs in all kinds of magnetic fields presented in [3], and can be understood analyzing the properties of these solutions to the solar neutrino problem. In this scenario, we need a strong suppression of the ^{7}Be neutrinos (similar to the small mixing angle solution in the MSW scenario) in order to accommodate both results from the Homestake and Gallium experiments (Sage, Gallex, GNO). So, for the ^{7}Be neutrino line we must have a completely adiabatic transition, which makes this line very stable against perturbations of the magnetic field profile.

But although we cannot use MHD perturbations to test the RSFP solution in Borexino, it has recently been discussed [20] how the low value of the expected rate of the beryllium line neutrinos on this experiment would be a clear indication of the RSFP mechanism.

4.1 The Hellaz and Heron experiments

These experiments [11,12] will utilize the elastic reaction, $\nu_{e,\mu,\tau} + e^- \rightarrow \nu_{e,\mu,\tau} + e^-$, for real-time detection in the energy region dominated by the *pp* and ^{7}Be neutrinos. They will both measure the energy of the recoil electron and the overall rate. These low energy neutrinos are the most abundant solar neutrinos, and the prediction of their flux is the one which carries less uncertainty, because of the correlation of these neutrinos with the solar luminosity. Since the MHD fluctuations we found in [3] appear to be affecting neutrinos with an energy range of the order of the *pp*-neutrinos energy, maybe Hellaz and/or Heron would be able to feel the time fluctuations on the neutrino signal generated by the MHD fluctuations.

We calculate the cross-section of the neutrino-electron scattering in the usual form [22], using a step function for the detector efficiency, to take into account the threshold in the electron kinetic energy ($T_{\mathrm{min.}} = 0.1\,\mathrm{keV}$). Since we do not have information about the resolution function of the detector, we assumed a perfect resolution (meaning that the measured kinetic energy of the scattered electron is the true one). So we calculate the total rates following the expression:

$$R = \int_{E_{\mathrm{min}}}^{E} \int_{T_{\mathrm{min.}}}^{T} \left[\frac{\mathrm{d}\sigma_e(T,E)}{\mathrm{d}T} P_{\mathrm{surv}}(E) + \frac{\mathrm{d}\sigma_x(T,E)}{\mathrm{d}T}(1 - P_{\mathrm{surv}}(E)) \right] \Phi(E)\mathrm{d}E\mathrm{d}T, \quad (13)$$

where $\Phi(E)$ is the solar neutrino flux and $\mathrm{d}\sigma_{e(x)}(T,E)/\mathrm{d}T$ is the differential cross-section of the electron (non-electron) neutrino elastic scattering with electrons, in terms of the neutrino energy (E) and the electron kinetic energy (T).

We present in Fig. 4a the expected detection rate in low energy neutrino experiments, with the value of $\Delta m^2 = 1.3 \times 10^{-8}\,\mathrm{eV}^2$, in terms of the neutrino energy (thus not performing the integration in the neutrino energy in (13)), for the maximum and minimum of the magnetic perturbations. We plot also the result with no perturbation, and for the SSM prediction.

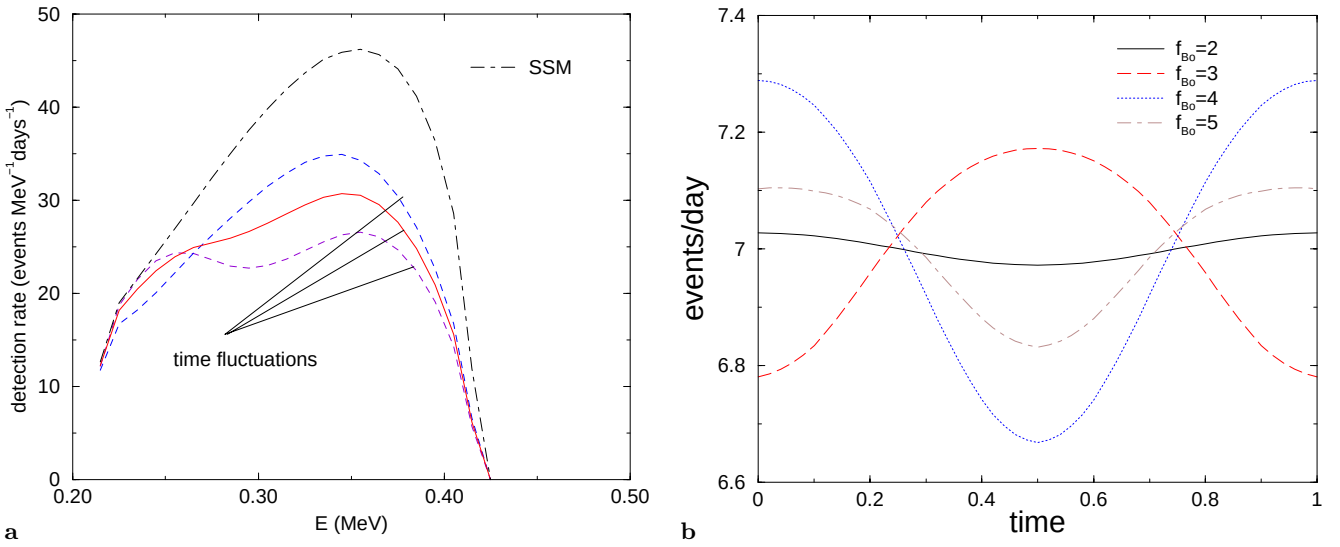

Fig. 4. a Expected rate detection in low energy neutrino experiments normalized to the standard solar model expectaction, as a function of the neutrino energy, assuming a perfect energy resolution, for no perturbation (*solid line*), and maximum perturbation (*dotted lines*), and **b** time variation of the total rates expected, in events/day, in low energy neutrino experiments

In Fig. 4b we present the time fluctuations of the total rates calculated for low energy neutrino experiments. We show the fluctuation of the number of events per day in one period of MHD fluctuations. In this scenario we expect a $\sim$ 8% fluctuation with a period of $\gtrsim 20$ days, where this last information is provided by the MHD equations. The total detection rate is expected to be ~ 7 events/day in Hellaz. We can present the result given in Fig. 4b in terms of the experiment running time that is necessary to identify such fluctuations. If we assume that there are no significant systematic errors, this time is given by the amount of days needed to reduce the statistical errors to a value lower than the expected sign variation. To do this estimation, we can split the total data sample into two samples, one around the maximum of the MHD fluctuation and the other one around the minimum. To identify the fluctuations we need the statistical errors of these data sample to be less than half of the perturbation amplitude. Since the statistical error is given by $1/(n^{1/2})$, where n is the number of events in the sample, we can write

$$\frac{\Delta R}{2} > \frac{1}{\sqrt{N/2}}, \tag{14}$$

where N is the total number of events recorded by the experiment, and ΔR is the maximum variation of the total rates, calculated as in (13). The factor 2 comes from splitting the number of events in two samples. Since we expect something around $\sim 7\,pp$ events/day on experiments like Hellaz or Heron, we can write for the number of running days needed to identify the fluctuations

$$N_{\rm days} > \frac{1}{7} \times 2 \left(\frac{\Delta R}{2}\right)^2 . \tag{15}$$

The result of this estimation is presented in Fig. 5. From this we can see that, for one year (365 days, or $\sim$ 2500 events) of data taking, in principle it is possible to distinguish such fluctuations in the Hellaz experimental results, if we have $3 \leq f_{B_O} \leq 5$.

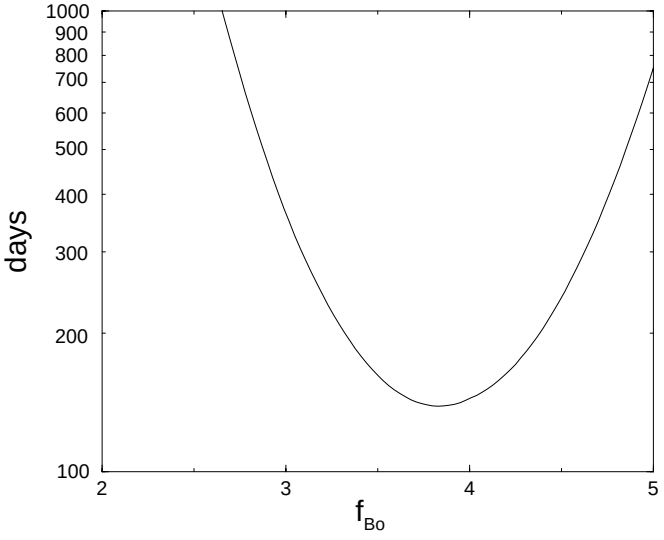

Fig. 5. The number of days needed to identify the MHD fluctuations of Fig. 4b (assuming zero systematic errors)

The magnetic field configuration used here is quite large for the convective zone (we are using f_{B_0} up to 4). We can decrease the value of the magnetic field without changing the solution to the SNP, if we increase by the same factor the neutrino magnetic moment. But changing the magnetic field will change the MHD fluctuations, changing the expected time fluctuations predicted to be seen by low energy experiments. If we decrease the magnetic field, we get fluctuations with a smaller oscillation length, and the parametric resonance felt by the solar neutrinos will occur for lower values of the neutrino energy.

In Fig. 4 we can see that the fluctuations achieve $\sim 8\%$ of the signal for $f_{B_0} = 4$, but decreases for $\sim 5\%$ with $f_{B_0} = 3$, and almost vanishes for $f_{B_0} = 2$.

5 Conclusion

The present data on solar neutrinos does not show any positive flux-independent indication of neutrino oscillation. For instance, the Super-Kamiokande experiment is not detecting a day–night asymmetry, nor a spectrum distortion of the neutrino flux. The only positive evidence of solar neutrino oscillations comes from the total rate detection on different solar neutrino experiments, and this scenario leaves room for a number of different possible mechanisms to solve the solar neutrino problem [19]. Finding new ways to distinguish these possibilities is then very important in order to reveal the true mechanism that is causing the observed solar neutrino deficit. If the RSFP is this mechanism, the analysis presented here is one of the few ways to distinguish it from other oscillation scenarios, and we showed that it is possible to find a signature of this mechanism on possible time fluctuations of the low energy neutrinos.

Acknowledgements. This work was partially supported by Fundação de Amparo à Pesquisa do Estado de São Paulo (FAPESP), Conselho Nacional de Desenvolvimento Científico e Tecnologógico (CNPq).

References

1. A. Cisneros, Astrophys. Space Sci. **10**, 87 (1970)
2. M. Voloshin, M.I. Vysotsky, L. Okun, Sov. J. Nucl. Phys. **44**, 440 (1986)
3. N. Reggiani, M.M. Guzzo, J.H. Colonia-Bartra, P.C. de Holanda, Eur. Phys. J. C **12**, 269 (2000)
4. K. Lande et al. (Homestake Collaboration), Astrophys. J. **496**, 505 (1998)
5. W. Hampel et al. (GALLEX Collaboration), Phys. Lett. B **447**, 127 (1999)
6. M. Altmann et al. (GNO Collaboration), Phys. Lett. B **490**, 16 (2000); C. Cattadori on behalf of GNO Collaboration, talk presented at TAUP2001, 8–12 September 2001, Laboratori Nazionali del Gran Sasso, Assergi, Italy
7. D.N. Abdurashitov et al. (SAGE Collaboration), Nucl. Phys. (Proc. Suppl.) **91**, 36 (2001); http://EWIServer.npl.washington.edu/SAGE/
8. S. Fukuda et al. (SuperKamiokande Collaboration), Phys. Rev. Lett. **86**, 5651 (2001); **86**, 5656 (2001)
9. Q.R. Ahmad et al. (SNO Collaboration), Phys. Rev. Lett. **87**, 071301 (2001)
10. L. Oberauer, Nucl. Phys. B Proc. Suppl. **77**, 48 (1999)
11. A. De Bellefon for HELLAZ collaboration, Nucl. Phys. B Proc. Suppl. 70, 386 (1999)
12. R.E. Lanou, Nucl. Phys. Proc. Suppl. **77**, 55 (1999); Proceedings of the 8th International Workshop on Neutrino Telescopies (Venice, Italy, 1999), edited by M. Baldo Ceolin, Vol. I, p. 139
13. J.P. Goedbloed, P.H. Sakanaka, Phys. Fluids **17**, 908 (1974)
14. M.M. Guzzo, N. Reggiani, J.H. Colonia Phys. Rev. D **56**, 588 (1997)
15. J.N. Bahcall, R.K. Ulrich, Rev. Mod. Phys. **60**, 297 (1988); J.N. Bahcall, M.H. Pinsonneault, Rev. Mod. Phys. **64**, 885 (1992); J.N. Bahcall, Neutrino astrophysics (Cambridge University Press, Cambridge 1989); J.N. Bahcall, S. Basu, M.H. Pinsonneault, Astrophys. J. **555**, 990 (2001)
16. M.M. Guzzo, H. Nunokawa, Astropart. Phys. **12**, 87 (1999)
17. O.G. Miranda, C. Peña-Garay, T.I. Rashba, V.B. Semikoz, J.W.F. Valle, Nucl. Phys B **595**, 360 (2001)
18. J. Derkaoui, Y. Tayalati, Astropart. Phys. **14**, 351 (2001)
19. A.M. Gaggo et al., Phys. Rev. D **65**, 073012 (2002)
20. E.Kh. Akhmedov, J. Pulido, Phys. Lett. B **485**, 178 (2000); Astropart. Phys. **13**, 227 (2000); Phys. Lett. B **529**, 193 (2002)
21. C.E. Ortiz et al., Phys. Rev. Lett. **85**, 2909 (2000)
22. J. Bahcall, M. Kamionkowski, A. Sirlin, Phys. Rev. D **51**, 6146 (1995)